Imaging of Placental Pathology

Prins, Jelmer Riemer; Sebire, Neil; Khalil, Asma; Gordijn, Sanne Jehanne

Published in:
Benirschke's Pathology of the Human Placenta

DOI:
10.1007/978-3-030-84725-8_32

Imaging of Placental Pathology

32

Jelmer Riemer Prins, Neil Sebire, Asma Khalil, and Sanne Jehanne Gordijn

Introduction to Placental Imaging

History

In 1958 clinical ultrasound examination was first described by the Scottish group of Ian Donald [35]. From the early 1960s, ultrasound has been used in obstetric practice, earliest clinical uses in obstetric care being determination of fetal position and placental localization. Prior to use of ultrasound examination, placental localization, mainly to exclude placenta previa, was performed by soft tissue X-ray, cystography, angiography, placentography (with the use of isotopes with radioactive sodium, iodine 131, or chromium 56), amniography, and thermography (infrared sensing, adequate for vertical localization) [18]. All these alternative techniques to visualize the position of the fetus or the placenta exposed the fetus and the mother to various degrees of radiation and radioactive materials or put them at risk by the use of complex and potentially dangerous invasive procedures. Initial reports of diagnosis of pathology (hydatidiform mole) were made in 1963, but it was not until 1968 that the placenta could be visualized at all positions [21].

Ultrasound

2D Technique for Placental Anatomy

The technique of antenatal diagnostic ultrasound examination is based on the principle of generating and reflecting high frequency, low intensity ultrasonic sound waves using a transducer composed of an array of piezoelectric crystals. The reflected sound waves are above the frequency that is audible by the human ear: >20,000 Hz. After transmission of the sound waves, the probe records the frequencies of the echoes reflected by tissues with different consistency and density resulting in different frequencies of the returning signal, from which an image representing different echo densities is generated. The earliest ultrasound images were static and lacked any gray scale [21], but in the 1970s real-time ultrasound scans were performed in which two-dimensional gray scale images are rapidly updated resulting in a "real time" display of the images (B mode), which remains the standard technique used in obstetric care.

Diagnostic ultrasound has been in use in obstetric care for more than five decades, but the placenta has historically received less attention than the fetus [10]. Similar to the approach to placental sampling for histopathology after delivery [68], the placenta should be systematically evaluated while still in utero by ultrasound examination; such sonographic evaluation has been proposed to include placental location, evaluation of size including measurement of thickness and/or volume, implantation, morphology, anatomy, and a search for anomalies.

Doppler Imaging for Blood Flow Evaluation

Assessment of placental blood flow and vascularity can be performed by the use of color Doppler imaging [10]. Color pulsed Doppler measured flow velocity evaluation has been possible from the early 1980s. Doppler measurement techniques make use of the frequency shift principle, that with moving structures (such as blood cells), the frequency that is reflected from the transmitted wave differs by frequencies dependent on the velocity and direction of the moving structure. These Doppler features can be made visible as colors reflecting blood flow superimposed on the gray scale anatomic image, usually with different colors being used for flow toward or away from the transducer. Furthermore,

J. R. Prins (✉) · S. J. Gordijn
University Medical Center Groningen, Department of Obstetrics and Gynecology, Groningen, The Netherlands
e-mail: j.r.prins@umcg.nl

N. Sebire
Great Ormond Street Hospital, London, UK

A. Khalil
St. George's Hospital, University of London, Fetal Medicine Unit, London, UK

R. N. Baergen et al. (eds.), *Benirschke's Pathology of the Human Placenta*, https://doi.org/10.1007/978-3-030-84725-8_32

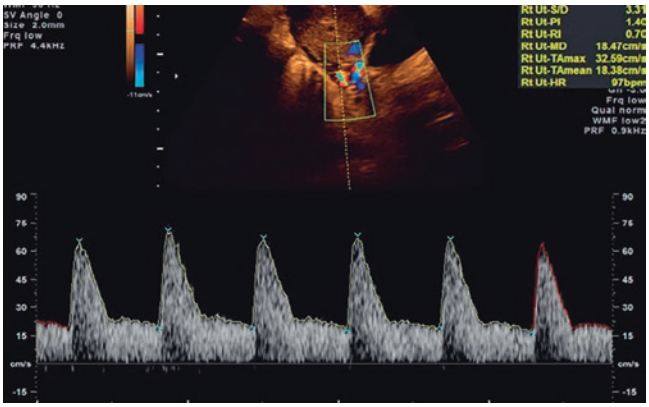

Fig. 32.1 Waveform from uterine artery [3]

pulsed waved Doppler may be used to determine flow within a specific vessel including determination of the pulsatility index (PI) (Fig. 32.1), that reflects resistance in the vessel, by using the flow velocity waveforms [21, 44, 93].

3D and 4D Ultrasound for Volumetric Evaluation

3D ultrasound uses volume rendering by using three spatial dimensions of ultrasound data and becomes 4D when a time dimension is added, appearing as a "real-time" 3D image. To generate a 3D volume of ultrasound data several techniques can be used, using either movement of the sonographers hands with the collection of transducer orientation data and/or mechanically with movement within the transducer [52].

The development of 3D ultrasound allows accurate reconstruction of the placental volume by using multiplanar VOCAL (virtual organ computer aided analysis) and spatial relationships [96, 129] and such 3D images can be used for a surface rendered analysis of the placenta, for example, the umbilical cord insertion and placental abnormalities (Fig. 32.2) [5].

3D power Doppler (3DPD) enables semi-quantitative and qualitative assessments of placental vascularization and flow patterns [131]. The method therefore potentially provides a new in vivo imaging tool for examining spiral artery development through pregnancy starting from the first trimester [119].

The most recent application in ultrasound is high-definition flow (HD flow), which visualizes bidirectional flow that may allow evaluation of the placental vascular tree since the signal is "cleaned" by the application of small sample volumes and provides optimal clutter elimination with adaptive wall filtering.

Safety of Ultrasound

Antenatal ultrasound examination is generally regarded as safe for fetal and placental imaging. However, ultrasound is

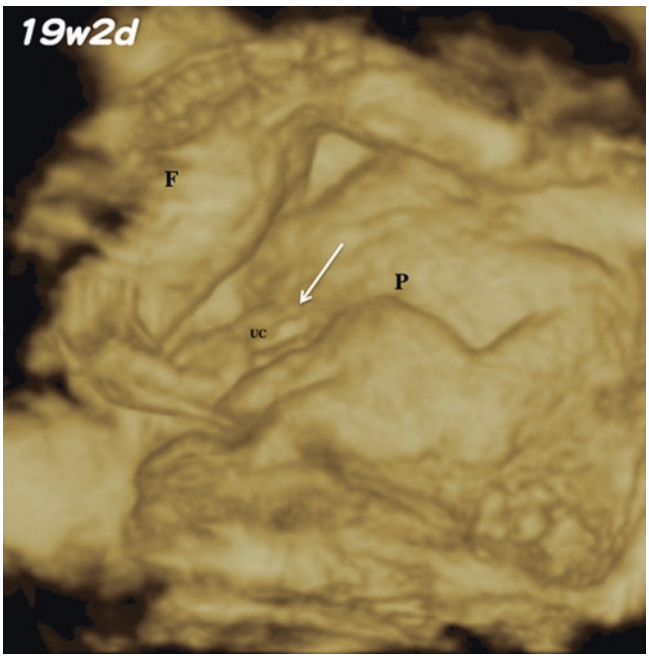

Fig. 32.2 Example of three-dimensional surface-rendered image of the placenta (P). The arrow indicates umbilical cord (UC) insertion into the placenta. F, fetus [5]

associated with some potential mechanisms that could theoretically cause adverse effects including thermal, non-thermal, and mechanical mechanisms [9].

Many studies, however, have shown an acceptable safety profile even in this susceptible population in pregnancy, prone for structural developmental damage. In a review of ultrasound safety, it was concluded that "The safety of obstetrical ultrasound is generally supported when used as medically indicated. The importance of the medical use of ultrasound by skilled and/or licensed sonographers or physicians is endorsed by American College of Obstetricians and Gynecologists (ACOG), American Institute of Ultrasound in Medicine (AIUM), and the food and drug administration (FDA)." However, the safety of modern advanced machines with higher output (mW/cm^2) and increasing use of Doppler, 3D, and 4D ultrasound (also with higher output) has not been fully confirmed by clinical studies [53].

MRI

Magnetic resonance imaging (MRI) as an imaging technique was reported in 1971 by Raymond Damadian and initially described as nuclear magnetic resonance (NMR) for the detection of tumors [29]. MRI represents a noninvasive imaging technique that produces cross-sectional images which allow reconstruction of detailed three-dimensional anatomical images with gray scales representing different densities of tissue, mainly based on the differences in water

and/or fat content of the tissues. The technique is based on the detection of changes in direction of protons in a rotational axis and uses powerful magnets that induce a strong magnetic field, thereby initiating protons in tissues to align with the field. When a radiofrequency current is then pulsed, protons spin out of equilibrium, straining against the pull of the magnetic field. After ceasing the radiofrequency pulse, the MRI sensors detect and record the energy released caused by the protons that realign with the magnetic field. Contrast agents (for example, gadolinium) can be given to a patient before or during the MRI to increase the speed at which protons realign with the magnetic field and thus create more energy resulting in a brighter image. MRI has been reported in pregnancy for almost 40 years [117]. But MRI in obstetrics is mainly used as a second line imaging modality for the evaluation of specific fetal anatomical structures in combination with ultrasound examination, as well as to improve the diagnosis of morbidly adherent placentae [73, 109].

Although MRI is promising for certain indications, the main focus of the chapter will be imaging of the placenta by ultrasound since MRI is not widely available, nor is the expertise to analyze the images and MRI remains expensive. MRI examination in pregnancy does potentially allow additional functional testing capacities, such as evaluation of microvascular parameters (dynamic contrast-enhanced (DCE) arterial spin labeling (ASL)), oxygenation (blood oxygen level dependent (BOLD), diffusion weighted imaging (DWI)), and metabolism (magnetic resonance spectroscopy). However, further research is required to better define the role of the MRI in evaluation of placental function, including use of ultrasound complemented by MRI [114].

One of the advantages of MRI is that the image quality is independent of common confounding factors affecting ultrasound examination, such as maternal obesity, fetal position (for example, presence of calcified bones close to the ultrasound probe), and lack of contrast due to oligohydramnios. However, MRI has a significant disadvantage, in the form of movement artifact due to fetal or maternal movements, both breathing movements and gross movements, which can limit the quality of images. MRI is not currently readily and widely available, nor are the required skilled interpreters specialized in placental MRI [19].

Turk et al. focused in their review on the quantitative measures of oxygenation through the placenta by MRI. They made clear that ultrasound does not provide direct measurement of placental function and only indirect estimations of vascular resistance measurement is possible that reflects microvasculature changes. They described in vivo and ex vivo MRI experiments and the use of blood oxygen level dependent (BOLD) MRI and relaxometry to map the oxygenation process in the placenta. They conclude that "the placenta presents numerous technical and physiological challenges that are unlike any other organ system, as motion is challenging and there are many complex interactions between the fetus and the mother. Thus, there is a long road before robust, reliable, and standardized approaches, with known diagnostic accuracy are available for phase 3 and 4 studies" [8].

A large study has been initiated to gain insight into these details: "The Human placenta project, placenta imaging project (PIP)": "Recently-developed placenta-specific magnetic resonance imaging (MRI) tools will be used to quantify maternal perfusion and oxygen transfer throughout pregnancy in 3 groups of human subjects: (1) non-smokers, (2) smokers, (3) individuals at high risk for adverse outcome. The objective of this work is to develop a new non-invasive clinical tool for early identification of placental dysfunction." The primary objective is to implement and optimize the following techniques: discriminant microstructure assessment based on diffusion imaging, MR elastography, and MR susceptibility and hyperoxia for placental imaging as well as optimizing a placental imaging protocol using conventional T1 and T2 weighted sequences. This work will also examine safety of a MR elastography (MRE) in assessing the human placenta (in non-pregnant subjects, animal models, and already delivered human placentae) and the role of oxygen inhalation MR technique to determine perfusion across the placenta in normal and abnormal pregnancies [40]. This project will hopefully provide useful data for future use of MRI in placenta imaging.

Safety of the MRI in Pregnancy

As with all imaging techniques in pregnant women, safety of MRI in pregnancy is important and has been subject of many studies [81]. In vitro studies have shown an effect of magnetic fields on cell functions and signaling [83], and moreover animal studies showed an effect of MRI exposure on fetal development such as reduced crown rump length (CRL) in early gestation, reduced fetal weights, and increased fetal losses [51, 81, 82, 85]. However, in these studies the fetuses were chronically exposed for hours, much more than routine clinical MRI duration would last and adverse effects have not been confirmed in human retrospective studies. To date series have reported no increased rates of adverse effects on birth weight or congenital abnormalities [25, 81, 103, 120]. A possible effect on the hearing of the developing fetus has been described and has received specific attention because of the acoustic noise generated by the MRI. However, in line with the results described above the retrospective cohorts have not confirmed hearing abnormalities in fetuses exposed to MRI [25, 56, 103, 120]. The exact effects of stronger magnetic fields (3T instead of the more common used 1.5T) and safety throughout pregnancy remain to be determined with long-term follow-up studies.

The safety of the use of gadolinium-based contrast agents (GBCAs) remains uncertain; it is however known that GBCAs cross the placenta [90, 95, 98], and therefore that the fetus is exposed to GBCAs. Several case series have looked into GBCA in utero exposure and have not reported any adverse effects of fetal GBCAs exposure; however, one cohort study with a 4-year pediatric follow-up showed slightly increased rates of neonatal death, and increased rates of any rheumatological, inflammatory, or infiltrative skin conditions [81, 103]. In general most guidelines state that the fetal and/or maternal benefits by using GBCAs to reach a prenatal diagnosis should be weighed against the possible fetal risks [81].

Physiology Assessed by Ultrasound Examination

Normal Development

The placenta is first identified sonographically as a thickened echogenic region around the gestational sac at approximately 9–10 weeks of gestation. Once the endovascular trophoblastic plugs in the spiral arteries resorb, maternal blood flow is established within the placenta at around 11–14 weeks of gestation which can be visualized with Doppler ultrasound examination. Prior to this gestation, trophoblast plugs only allowed a small amount of blood and plasma to seep through [126]. The placenta is easily visualized from 14 to 15 weeks for evaluation of location and shape as a relatively homogenous gray area adjacent to the uterine tissue. The location is determined by a sagittal view for the posterior versus anterior location. Most placentas are implanted in the fundus to mid uterus and positions are typically described as anterior, posterior, left lateral, or right lateral. Assessment of the placental location in relation to the internal cervix is also made [65]. The shape of the placenta is determined by the area of persistent chorionic villi and is usually discoid. In general, in obstetric practice placenta size measurements are not routinely performed, only when the placenta seems to be abnormal by subjective visual evaluation. The normal thickness of the placenta is correlated with gestational age with approximately 1 mm additional thickness per week of gestation [24].

The third trimester placenta is less homogenous in appearance and shows echolucensies and calcifications. Calcifications are most often seen as echodensic "speckling" usually near the basal plate and septa and are a normal feature of placental maturation. Local calcifications may be due to infarctions and calcifications are also described in as plaques of perivillous or subchorial fibrin [111].

On MRI, during gestation, the placenta shows similar changes to those described with ultrasound examination. The placenta appears homogenous in early mid pregnancy. In late mid pregnancy lobules are visible and from 36 weeks stratification of lobules is observed (Fig. 32.3). The ratio of placental and fluid signal intensities decreases with advancing gestational age [15].

(Common) Placental Lesions

Correlation of placental pathology with prenatal ultrasound features largely depends on the type of lesion, how big the lesion is, and the ultrasound-delivery interval. Many sonographic features are nonspecific and may be due to a range of different underlying pathologies, although some entities have reasonably specific appearances and examples are provided below [111].

Gestational Trophoblastic Disease (Chap. 28)

Gestational trophoblastic disease (GTD) comprises proliferative disorders of pregnancy involving placental (trophoblastic) tissue. GTD ranges from pre-malignant molar pregnancies (partial and complete hydatidiform) to malignant gestational trophoblastic neoplasia (GTN). GTN includes invasive mole, choriocarcinoma, and placental site and epithelioid trophoblastic tumors; the latter are rare [64].

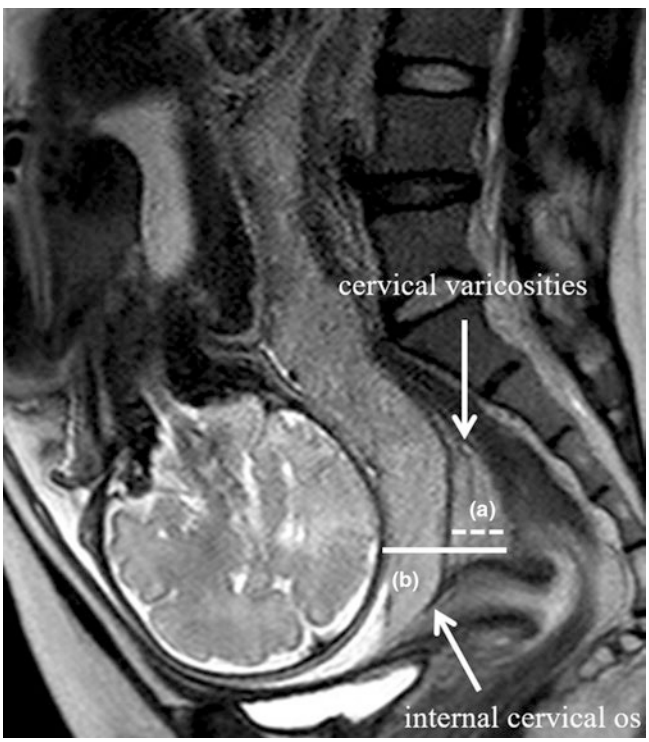

Fig. 32.3 Example of MRI of placenta, in this case analysis because of possible placenta previa. Distance shown from most dorsal cervical varicosities to the deciduous side (**a**) and amniotic side (**b**) on T2-weighted sagittal slices containing the internal cervical os [6]

A molar pregnancy is characterized by abnormal villus development with associated trophoblast overgrowth and ultimately formation of hydropic villi appearing as "grape-like" cysts. Molar pregnancies are divided into complete and partial moles, with different genetic, clinical, and sonographic characteristics, usually partial molar features being more subtle [23]. In addition, molar pregnancies can appear with a coexistent healthy fetus in the form of a co-twin or rare mosaic.

On routine ultrasound examination, complete molar pregnancy is often characterized by diffuse hydropic swelling of the villi, seen as diffuse cystic spaces in the placenta with no embryo or fetus [23, 112] (Fig. 32.4). It has been shown that these cystic changes become apparent from the second month of gestation onwards but are reliably detected from around 12 weeks [14, 60]. Due to the high HCG levels sometimes hyper stimulated ovaries with large lutein cysts can be seen, although this is rare in early pregnancy.

Partial molar pregnancies are characterized by patchy cystic changes in combination with abnormalities of the placenta, decidua, or myometrium, often fetal or embryonic elements are present [23]. The rare late partial molar pregnancies are characterized by an enlarged hydropic placenta in combination with a (triploid) fetus with typical severe abnormalities; these include fetal growth restriction, cardiac abnormalities, syndactyly, short limbs, and central nervous system (CNS) abnormalities.

The majority of gestational trophoblastic neoplasias are thought to be developed in association with a molar pregnancy. However, rarely choriocarcinoma develops in apparently normal pregnancies. Intraplacental tumors have been described in relation to adverse outcomes, and are most often diagnosed after birth [64, 113].

MRI is not usually needed in the evaluation of molar pregnancies, although in atypical presentation of molar pregnancies MRI can be used [77], this could especially have additional value regarding the need for additional invasive testing or planning for delivery mode in the rare case of a molar pregnancy with a coexisting twin fetus [12, 54]. MRI is, however, useful in the evaluation of malignant (gestational) trophoblastic tumors.

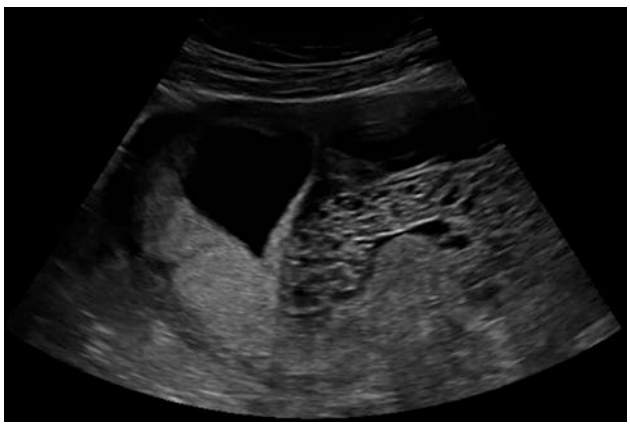

Fig. 32.4 Example of ultrasound image of hydratiform mole pregnancy

MVM (Chap. 13)

Maternal vascular malperfusion, historically referred to as uteroplacental underperfusion, placental bed pathology, or utero placental insufficiency, indicates the abnormal, shallow implantation of the placenta with inadequate spiral artery remodeling due to impaired invasion by trophoblast, resulting in abnormal maternoplacental blow flow and subsequent high resistance circulation in the placenta. Shear stress of abnormal pulsation flow on villi may cause further damage and subsequent pathologies. MVM is usually clinically recognized prior to birth and can be characterized by histopathological placental investigation post-delivery, as the most common cause of fetal growth restriction (FGR) and pre-eclampsia (PE) [68, 86]. Several placental features are considered to be indicative of MVM, some of them more or less detectable by ultrasound such as distal villous hypoplasia, placental infarcts, and retro placental hemorrhage. This lesion is, however, most often diagnosed not by direct evaluation of the placenta, but by the measurement of its effects on the fetus and mother. Declining fetal growth, or size below a certain cut-off, usually the tenth percentile (p10) of a reference population/standard, is considered to be a sign of fetal growth restriction due to impaired implantation. In addition, other features of abnormal placental function are measurements of Doppler abnormalities and part of the abnormal measures that define FGR [46]. Doppler measurements to estimate the placental vascular resistance and function can be measured in both mother and the fetus. Maternal ultrasound using Doppler measurements are performed in proximal uterine arteries, and MVM is associated with bilateral high resistance notched waveforms. Fetal measurements are most often performed in the umbilical arteries, but also middle cerebral artery (MCA), ductus venosus (DV), and aorta isthmus. In early FGR, absent end diastolic and reversed end diastolic flow in the umbilical arteries indicate increased fetoplacental resistance and that the fetus is in suboptimal condition. A low PI in the MCA indicates redistribution of blood toward the more vital organs ("brain sparing") [110]. A negative wave in the DV indicates cardiac decompensation in early FGR. Vasodilation in the MCA combined with aortic isthmus retrograde flow confers a high risk of acquired brain injury in case of placental insufficiency. Late FGR has less prominent umbilical artery abnormalities; usually absent end diastolic flows are not observed.

Parenchymal Infarction

Parenchymal infarction can be detectable on ultrasound, although a low detection rate antenatally is described. Infarctions can be seen typically near the maternal surface and are more easily visualized when complicated by hemorrhage [49]. The appearance of infarctions depends on the degree of hemorrhage, the interval between infarction and ultrasound, and how large the infarction is. It has been described as initially a hypoechoic lesion that becomes with increasing time more echogenic, sometimes visible as a hyperechoic mass and sometimes with calcifications [49, 59]. Cooley et al. defined the ultrasound appearance of the infarct as an echo poor lesion with characteristic halo surround [27].

MRI can detect infarcts as well as hyperintense lesions on T2-w sequences. In one series of placentas with infarctions at gross examination post-delivery, the antenatal detection rate of infarction by MRI was high with a sensitivity of 96% and a specificity of 63%. In contrast to the ultrasound that only measures the vascular disease when Doppler flows become abnormal after vasoconstriction and secondary changes exceed a certain threshold [13], MRI is suggested to be able to detect possible changes at an earlier stage [84, 88].

Retro Placental Hemorrhage/Abruption

Retro placental hemorrhage may be difficult to detect by ultrasound, and even when suspected clinically only about one-third of lesions are visualized [45]. Acute retro placental hemorrhage appears as a slightly hyperechoic area between placental tissue and the uterine wall. Abruption/RPH is described as hyperechoic to isoechoic when compared to the placenta in the acute phase. Once the hematoma begins to resolve the lesion appears more hypoechoic after approximately 1 week and sonolucent after around 2 weeks [97]. A thick placenta as a solitary finding is also described. A specific feature "jello" sign has been described, indicating a specific movement ("jiggling") of the placenta once sudden pressure is applied. Ultrasonographic criteria have been summarized to include pre-placental and retro placental collection, "jello-like" movement, marginal, intra-amniotic, and subchorionic hematoma and increased heterogeneous placental thickness (more than 5 cm in perpendicular plane) [100]. Color Doppler sonography may be helpful to differentiate clot from the uterus or placenta since the hematoma will not contain vessels or blood flow. In some cases septations may be seen in large subacute hematoma or even the presence of fluid–fluid levels [130].

Intervillous Thrombus/Placental Lake

Coagulation of blood in the intervillous space can result in various pathologic lesions that appear in a different way on ultrasound. Most have a laminated appearance and displace adjacent villi, resulting an echodensic border. They have been described in relation to MVM; due to the inadequate adaptation of spiral arteries, the velocity of the maternal blood flow is higher than in normal pregnancy and is suggested to drive apart the villous branches and rupture the anchoring villi displacing surrounding anchoring villi [20]. Often they are not a solitary finding and are often of uncertain significance [57].

Placental lakes are seen as small echo poor areas within the placental parenchyma and are usually considered to be harmless when referred to as the small anechoic areas at the center of a cotyledon in normal term placentas and normal parenchymal tissue surrounding the lakes [104]. They can be visualized on ultrasound as anechoic or hypoechoic lesions. They are thought to be areas within the parenchyma with a low maternal flow and/or villus poor areas of intervillous space. The fetal and maternal placental vessels in relation to the lake including the placental lake itself can be visualized with 3D high definition flow [55]. The significance of placental lakes remains unclear and, in the literature, conflicting results are reported. It has been suggested that the significance depends on the gestational age of appearance, the number, and size of the lesions [48].

Subchorionic Thrombohematoma (Breus' Mole)

A large maternal blood clot that separates the chorionic plate from the villous chorion is also called massive subchorionic thrombohematoma (or "Breus" mole) (Fig. 32.5). It is a rare lesion that has been reported in association with adverse perinatal outcomes. It is not a molar pregnancy but the appearance of coagulated blood mimics in some ways the appearance of the villous degeneration in moles [1, 37]. Dependent on localization the thrombohematoma has more or less consequences, for example, the clot can result in compression of the cord or venous flow. On ultrasound the thrombohematoma is visualized as a mass either heterogeneous or homogeneous with mixed high and low echogenicity, distinct from the normal ultrasonic texture of the placental parenchyma. The lesion can also present as placentomegaly [41, 87]. MRI and color Doppler are reportedly useful to differentiate "Breus" mole from other placental masses such as placental mesenchymal dysplasia and chorangioma, although no specific findings of "Breus" moles are described [1, 78].

Subchorionic thrombi and retro placental hematoma are also well visualized on MRI in T1 w sequences. Dependent on the interval until MRI the lesions may have a layered or

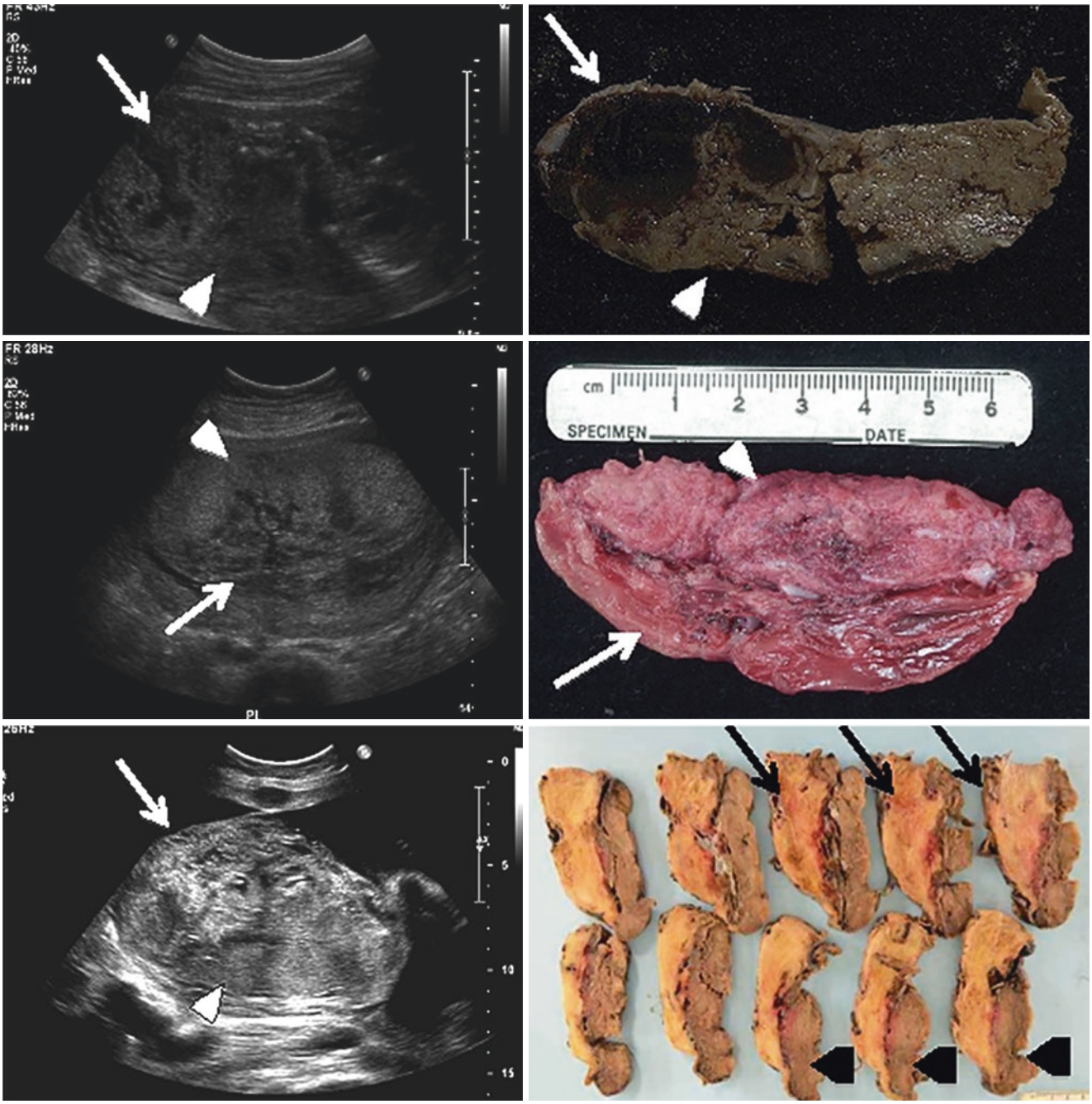

Fig. 32.5 Example of ultrasound (left panel) and gross pathology findings (right panel) of subchorionic thrombohematoma (Breus mole). Arrows indicate areas of hemorrhage identified beneath the chorionic plate (CP). Arrowheads indicate normal villous tissue with a granular appearance. BP basal plate [1]

laminated appearance. Venous stasis or thrombotic changes may cause hyper intense signal changes [78, 84].

Small Placenta (Placenta Hypoplasia)

Placenta hypoplasia is usually defined as placenta weight below p10. This correlates with placental size. Although not routinely performed on antenatal ultrasound placental size can be measured antenatally but the clinical significance remains undetermined. The normal thickness of the placenta is correlated with gestational age with approximately 1 mm per week of gestation [24]. The MRI would be suitable for volumetry [78].

Circumvallata

This represents a form of abnormal placentation in which the chorionic plate is smaller than the basal plate, resulting in the edges of the placenta appearing to roll inwards, with mem-

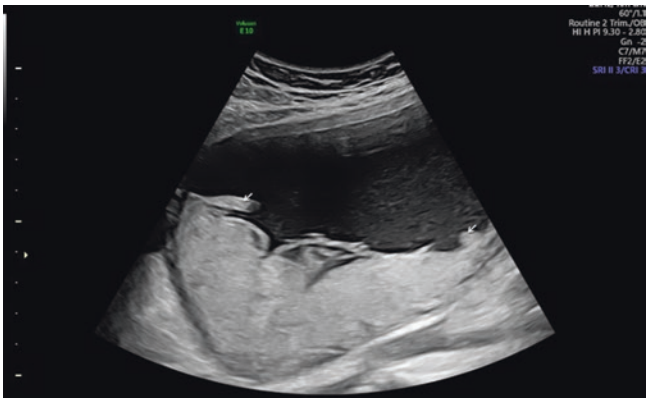

Fig. 32.6 Example of placenta circumvallata. Arrows at edges which appear to roll inwards

branes inserted from the inside toward the edge of the placenta (Fig. 32.6). This can be visualized on ultrasound as cylindrical, thickened membranes, the "tire" sign (peripherally) [130]. Clinically a circumvallate placenta is described with vaginal bleeding, associate preterm delivery (often due to preterm prelabor rupture of membranes), oligohydramnios, fetal growth restriction, abruption, and fetal death [121, 122].

Other Placental Parenchymal Abnormalities (Chaps. 16 and 29)

Placenta Mesenchymal Dysplasia (PMD)

PMD is a rare placental mesenchymal/vascular abnormality characterized by placentomegaly, cystic vesicles, and dilated chorionic blood vessels [11] (Fig. 32.7). PMD has an estimated incidence of approximately 1/4000 although the exact incidence is hard to determine as there may be underreporting. In a systematic review, combined with institutional findings the features on ultrasound were described. Most commonly, the placental abnormality was a cystic placenta with hypoechoic areas (80%), enlarged and/or thickened (50%), and/or with dilated chorionic vessels (16%). In the literature, authors often used descriptions such as "Swiss-cheese" or "moth-eaten" or terms as molar when characterizing the placenta sonographically [92]. The differential diagnosis with partial molar and complete hydatiform pregnancy on ultrasound features can be hard to make as the characteristics of the lesions closely resemble each other. However, PMD is usually associated with diffuse changes admired with normal placental parenchyma and a normal fetus. There is no risk of malignant trophoblastic disease in contrast to molar pregnancies [125]. Since some cases of PMD may be associated with underlying fetal syndromes such as Beckwith-Wiedemann syndrome, in addition to placental abnormalities, in a minority of cases abnormalities pertaining to the fetus

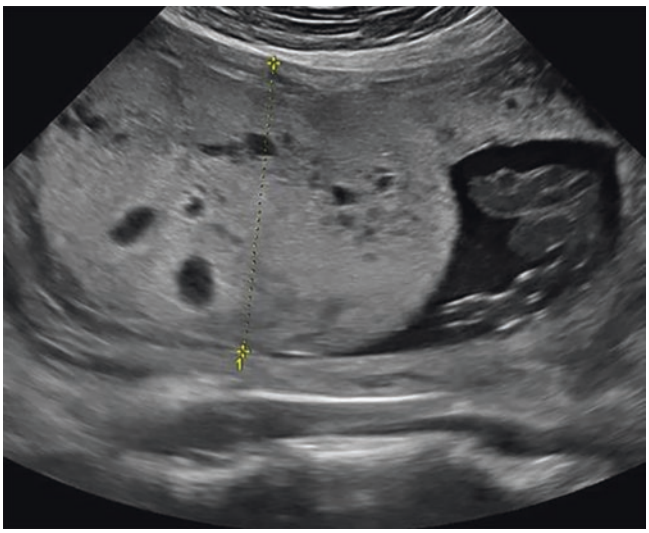

Fig. 32.7 Example of ultrasound image of placenta mesenchymal dysplasia

were described, such as large-for-gestational age, omphalocele, and organomegaly of the kidneys and liver. Intra-abdominal masses or hepatic cysts were the most commonly diagnosed isolated structural anomalies. The laboratory findings indicated an increased human chorionic gonadotrophin (HCG), hampering the differential diagnosis with molar pregnancy [92].

Chorangioma

A chorangioma is a placental hemangioma, composed of capillary-vascular channels with variable amount of intervening perivascular stroma, containing fibroblast, macrophages, and fibrous tissue [115]. Chorangiomas are often small and asymptomatic. Using ultrasound chorioangiomas appear as hypoechoic masses, often located adjacent to the placental cord insertion [62]. The size of the chorioangioma determines its consequences, the larger the chorangioma, the larger the fetal blood flow. Larger tumors (>5 cm) are associated with a hyper-dynamic fetal circulation [28]. Sometimes, vascularity pulsating at fetal heart rate using Doppler can be found. Once diagnosed it is recommended to assess polyhydramnios and fetal anemia by fetal middle cerebral arterial Doppler assessment [62].

Twin Pregnancies: Twin-to-Twin Transfusion Syndrome (TTS)/Twin Anemia Polycythemia Syndrome (TAPS) (Chap. 18)

Placental and umbilical cord abnormalities are more common in multiple pregnancy, in particular placenta praevia, vasa praevia, complete hydatiform mole and placental mes-

enchymal dysplasia, single umbilical artery, velamentous cord insertion, abnormal coiling, cord entanglement, and proximate cord insertions in particular in monoamniotic twin pregnancies. Most of these pathologies have already been described in this chapter.

Monochorionic twin placentas show characteristic vascular anastomoses. There are three types of vascular anastomoses: arterio-arterial (AA), veno-venous (VV), and arterio-venous (AV) anastomoses. AA and VV anastomoses are superficial, bidirectional, and have a low vascular resistance, while AV anastomoses are deep, unidirectional, and have a high vascular resistance. AA and VV anastomoses form direct connections between the two fetal circulations, while AV anastomoses consist of an artery from one twin and the vein of the other twin that are connected by a capillary network in a shared cotyledon below the chorionic plate. They are often seen as a supplying artery and a draining vein that pierce the chorionic plate in close proximity to each other. As a result of the unidirectional flow in AV-anastomoses an imbalance in the net transfusion of blood can occur. These anastomoses cannot easily be detected by ultrasound and are typically seen after delivery on macroscopic examination of the fetal side of the placenta or color dye injection of the vessels. The latter is particularly useful in minute anastomoses which might not be easily visualized by the naked eye.

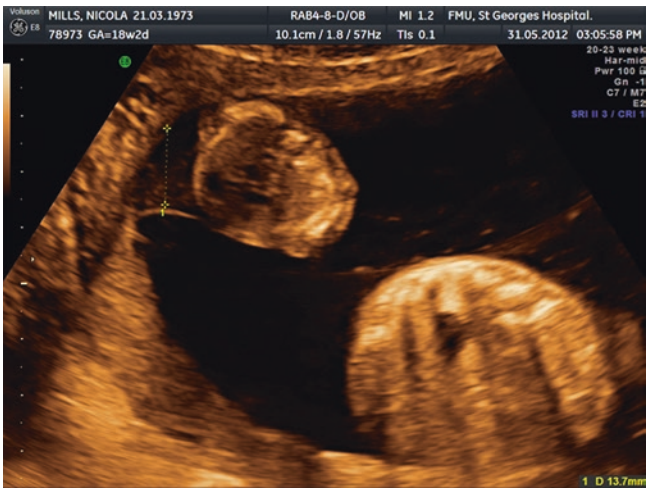

Fig. 32.8 Ultrasound image of significant amniotic fluid imbalance

The ultrasound diagnoses a vascular abnormality in the twin placenta, resulting in a net imbalance of blood flow across the vascular anastomoses is by diagnosing the clinical syndromes of TTTS or TAPS. TTTS requires the presence of significant amniotic fluid imbalance (Fig. 32.8). The "donor" twin has a deepest vertical pocket (DVP) of <2 cm (oligohydramnios) and the "recipient" twin has a DVP ≥8 cm (polyhydramnios) (Fig. 32.9). In Europe the diagnosis of polyhydramnios is ≥8 cm at ≤20 weeks and ≥10 cm after 20 weeks' gestation [67]. The diagnosis of polyhydramnios prior to 18 weeks has been proposed to use DVP ≥6 cm [66]. TTTS is associated with perinatal loss and significant neonatal morbidity; if untreated, it leads to fetal demise in up to 80–90% of cases, with morbidity rates in survivors of over 50% [105, 106].

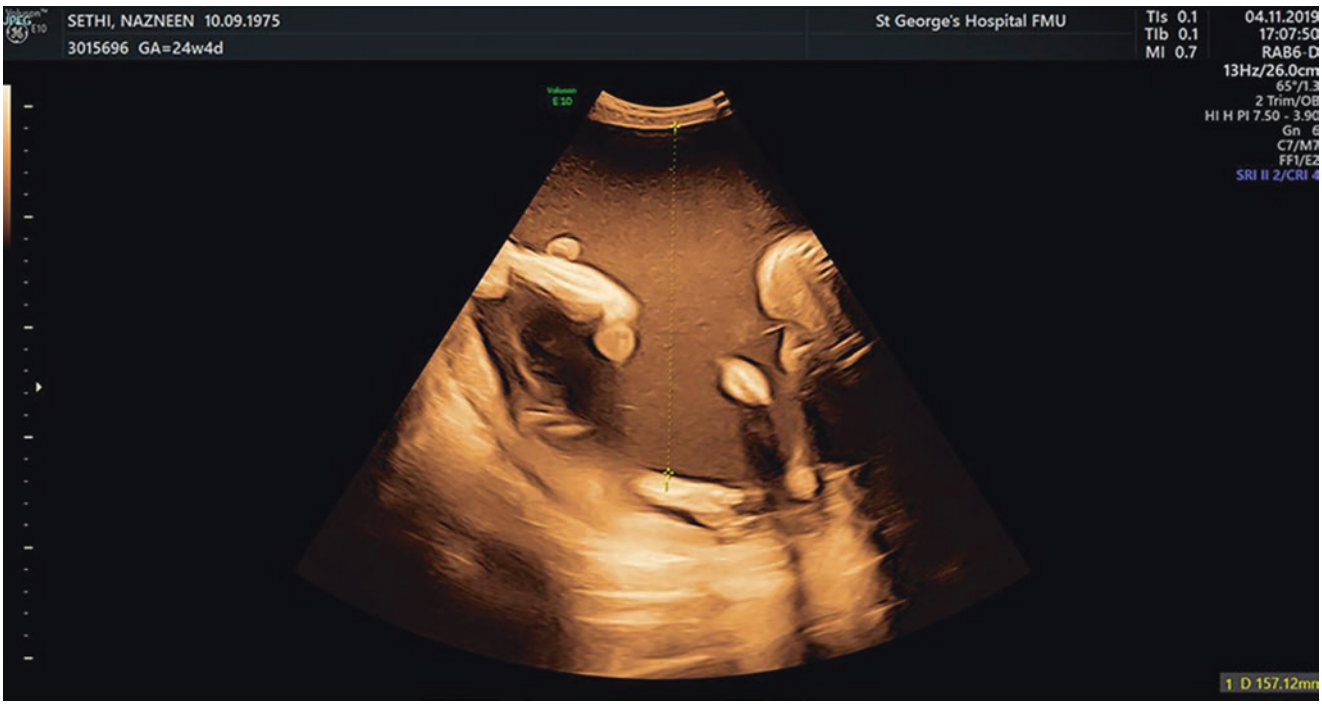

Fig. 32.9 Ultrasound image of significant polyhydramnion, in this case a pocket of 157 mm is measured

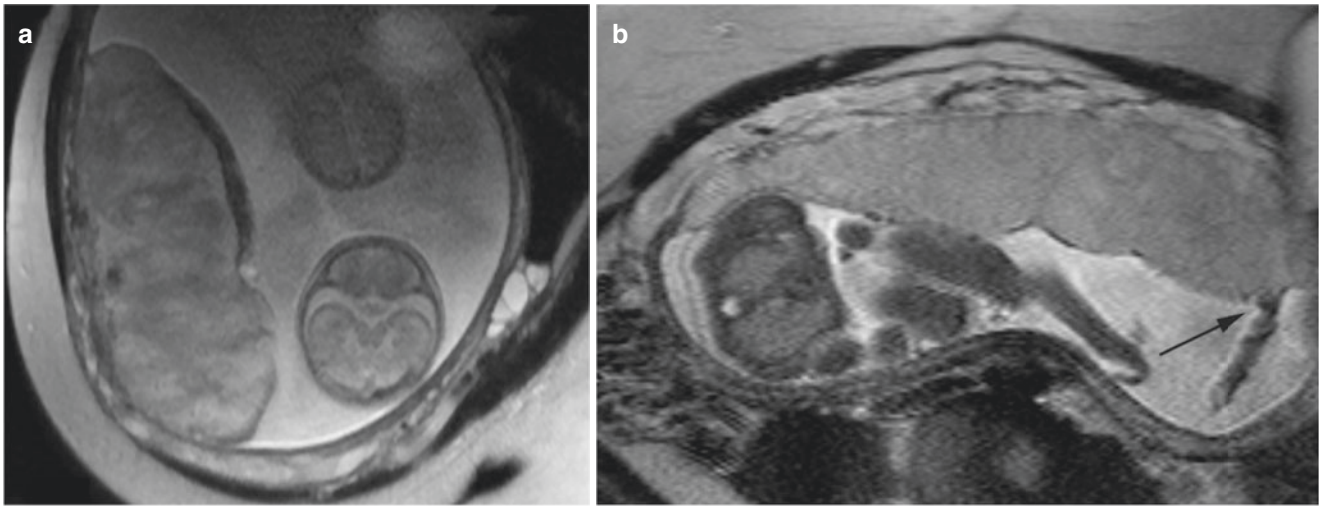

Fig. 32.10 Placental maturation. (**a**) T2-w image at GW 20 of a TTTS pregnancy in the sagittal plane, showing inhomogeneities with hyperintense patchy structures, including 100% of tissue, pathologically altered for this respective gestational age. (**b**) T2-w MRI of a non-TTTS pregnancy at GW 22 in the axial plane, showing normal placental maturation. Note the marginal cord insertion (arrow) of twin II (IUGR <10th percentile) [7]

In TTTS placentas there is an increase in velamentous cord insertion and unequal placental sharing, which is reported to be twice as common as in uncomplicated monochorionic [31]. It is also reported that there is often a color difference [94], which is thought to be due to differences in intraplacental blood volume and villous vascularity.

At present the gold standard for diagnosis of TTTS in twin pregnancies is ultrasound. MRI studies of the placenta in these pathologies have demonstrated abnormal maturation (Fig. 32.10). Histologically, placental maturation is represented by branching and the development of sinusoid capillaries in terminal villi, which can produce distinct signals on MR [15]. Placental maturation reported in TTTS could be the result of fetal hypoxia (as a consequence of fetoplacental malperfusion, reduced oxygen extraction from the placenta typically results in an intraplacental pO_2 that exceeds normal values, which inhibits villous growth) and/or growth restriction (which is associated with accelerated maturation of the placenta [71]).

TAPS is believed to be due to the presence of miniscule AV anastomoses (less than 1 mm) which allow slow transfusion of blood from the donor to the recipient, leading to highly discordant hemoglobin concentrations at birth. The postnatal diagnosis of TAPS is made based on the finding of chronic anemia (including reticulocytosis) in the donor and polycythemia in the recipient. The traditional criteria for diagnosis include a difference in hemoglobin concentration between the twins of more than 8 g/dl and reticulocyte count ratio greater than 1.7 or small vascular anastomoses (<1 mm in diameter) in the placenta [80, 116]. The prenatal diagnosis of TAPS is based on the finding of discordant middle cerebral artery (MCA). Doppler abnormalities, including an MCA peak systolic velocity (PSV) more than 1.5 multiple of median (MoM) in the donor, suggesting fetal anemia, and an MCA PSV less than 1.0 MoM in the recipient, suggesting polycythemia [67].

Additional ultrasound findings in TAPS include differences in placental echogenicity and thickness with a bright, thickened section for the donor twin and an echo lucent thin recipient section. The polycythaemic twin might have a starry sky appearance of the liver pattern due to diminished echogenicity of the liver parenchyma and increased brightness of the portal venule walls [80, 116].

Another observation is the striking difference in color between the plethoric placental share of the recipient and the pale placental share of the donor [123, 124]. This difference is usually pathognomonic of TAPS and may help differentiate TAPS from acute peripartum TTTS when there is unexplained large hemoglobin difference at birth [124].

Placentas in Selective Fetal Growth Restriction (sFGR)

In dichorionic twin pregnancies the evidence suggests that pathological associations may differ between small for gestational age (SGA) dichorionic twins and SGA singletons. Marginal and velamentous cord insertions appear more common in dichorionic twins, while maternal vascular malperfusion and fetal vascular malperfusion appear less frequent [69].

sFGR in a monochorionic twin pregnancy results primarily from unequal placental sharing. Typically, the growth restricted fetus often has a small placental share and a velamentous cord

insertion, while the larger fetus has a larger placental share and a (para-) central cord insertion. There are three types of sFGR in a monochorionic twin pregnancy according to the Gratacos classification. The placental characteristics vary according to the type of sFGR [47, 74]. Type I sFGR are characterized by the invariable presence of an average sized AA and mild to moderate unequal sharing; this appears on Doppler ultrasound as waveform pattern with positive end diastolic flow in the umbilical artery. Type II is also characterized by unequally shared placenta, but AA anastomoses may be absent or small, visible with Doppler ultrasound as a waveform pattern that shows continuous absent or reversed end diastolic flow in the umbilical artery. Type III sFGR placentas have larger AA anastomoses (almost double the size compared to type I) and a higher degree of sharing discordance visualized with Doppler ultrasound as intermittent absent or reversed end diastolic flow alternating with short periods of positive end diastolic flow in the absence of maternal or fetal breathing movements [4] (Fig. 32.11). In summary, the principal placental characteristics identified in sFGR in a monochorionic twin pregnancy are unequal placental sharing and velamentous cord insertions [31, 32, 39, 74, 79].

Placenta Accreta Spectrum (Chap. 14)

Ultrasound

Abnormally invasive placentas are nowadays often described using the term placenta accreta spectrum (PAS); these include placenta accreta, placenta increta, and placenta percreta [61]. The reported prevalence of PAS varies largely, also because of different diagnostic criteria and possibilities. After delivery often detailed histopathologic analysis is used for confirmation of PAS, and before birth both MRI and ultrasound are used for diagnostic workup. Unfortunately, no single imaging feature has been shown to be diagnostic for PAS [62]. The ultrasound features that are reported include the presence of multiple placental lakes with irregular margins, the loss of retro placental space between the placenta and myometrium, the presence of placenta previa, heterogeneous placental appearance, asymmetry of placental thickness, myometrial thinning, bladder wall abnormalities, and myometrial and bladder wall hyper vascularity [62]. The performance of antenatal ultrasound and the specific signs is not consistent in literature and depends on the exact criteria used.

MRI

The MRI offers a complete view of the placenta and besides that the possibility to visualize the maternal pelvic organs in relation the uterus and placenta [17]. When the placenta is in posterior position, or for other reasons making it difficult to visualize, such as maternal obesity, MRI may play an important role, in addition to evaluation of when morbid adherent placenta (accrete, increta, and percreta) is suspected [58]. Both direct and indirect signs of abnormal placental invasion have been described. The most obvious direct sign is a visible invasion of the placenta in the myometrial wall or disruption of the normal myometrial presentation which is trilaminar (hypo–hyper–hypo intense). The hyper intense area reflects the well-vascularized inner myometrial part. However, it can be challenging to accurately visualize the continuous myometrium and there is a significant risk of false positive cases [70]. A focal bulge or widening of uterine segment at the lower uterine segment or extra uterine invasion are other direct signs of abnormal placentation, with the most severe (placenta increta or percreta) indicating disruption of the uterine wall, changing its morphology and/or penetration of placental tissue in the uterus or surrounding organs [75]. The serosa of the uterine wall may be deviated but intact. The surrounding organs in the maternal pelvis should be visualized because a crucial step in the interpretation of findings is the identification of normal fat planes that separate the uterus and cervix from the adjacent rectum and bladder. Bladder involvement should be considered especially with placenta previa and cesarean section or other intra uterine surgery in the obstetric history. The bladder has a hypodense appearance on MRI, and thinning or irregularity of the wall sometimes accompanied by blood products in the lumen suggest bladder invasion by the placenta. The accuracy (based on expert opinion) of bladder invasion is very high, as well as the accuracy of the placental bulge [63].

Indirect signs include placental heterogeneity and asymmetric shape, and with lower accuracy, T2 hypo intense parenchymal bands in the perpendicular, hyper vascularization with very abnormal, tortuous intraparenchymal vessels, and enlarged pelvic veins [17].

Placenta Previa, Membranous Vessels, Vasa Previa (Chap. 17)

In most cases the placenta implants into the upper uterine body. However, in some cases implantation is in the lower segment and may even cover the cervix. Based on its exact location different subtypes are characterized. Since it is known that a majority of low-lying placentas “resolve” in relation to uterine growth and internal cervical os positioning, it is often stated that definitive diagnosis should be made around week 34 of pregnancy. With low lying placentas, the placental parenchyma may not cover the cervical os but intramembranous blood vessels may run in this area. In case of vasa previa the vessels are located close to the cervix. As these vessels are only protected by the membranes they are

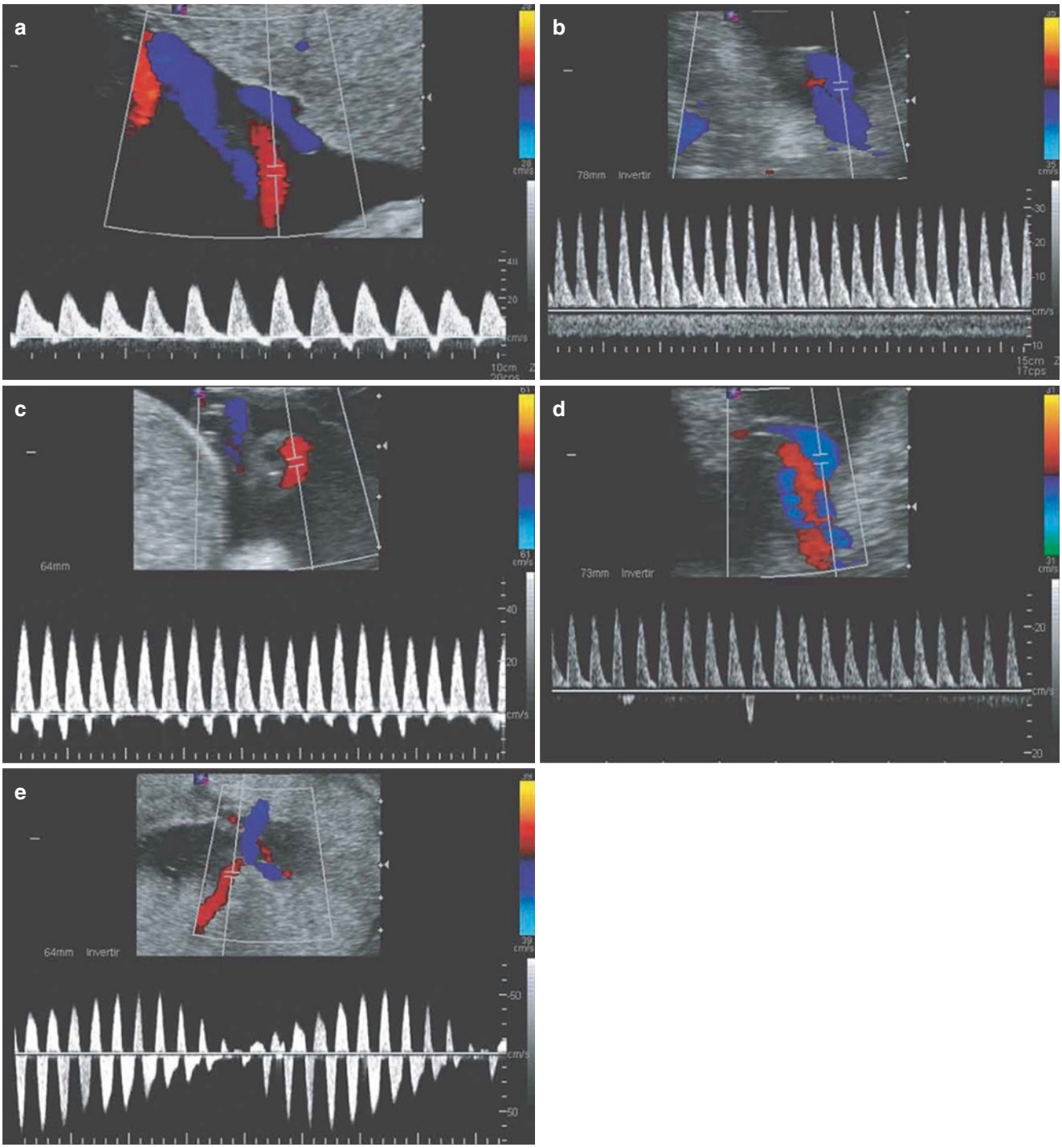

Fig. 32.11 Different umbilical artery Doppler waveforms in monochorionic fetuses with selective intrauterine growth restriction and intermittent absent or reversed end-diastolic flow (iAREDF). (**a**) Typical image of iAREDF with cycles showing absent and/or reversed flow. (**b**, **c**) Using the fastest sweep speed allows better appreciation of the cyclical nature of the changes, as present in most cases, which may range from (**b**) absent to (**c**) clearly reversed diastolic waveforms. The systolic waveforms also show a characteristic oscillating aspect which results from the influence of the transmitted waveforms in the peak velocity. (**d**) In a proportion of cases, the intermittent appearance of absent or reversed waveforms is not cyclical and follows a more irregular pattern, occasionally appearing irregularly over periods of minutes rather than seconds. (**e**) The large placental arterioarterial anastomoses causing this Doppler phenomenon can virtually always be found and insonated, showing the characteristic bidirectional and periodic pattern resulting from the collision of the two systolic waveforms (Gratacos et al. 2007)

vulnerable and have increased risk of rupture during delivery especially with artificial rupture of membranes.

Ultrasound

Regarding placenta previa, transvaginal ultrasound is the method of diagnosis and provides good views of the precise placental location in relation to the cervical canal. As placenta previa is a risk factor for abnormal placentation, this should also be evaluated by Doppler flow measurements.

In case of vasa previa, color Doppler should be used, often via transvaginal ultrasound. As maternal vessels at the edge of the placenta can mimic vasa previa, the waveforms should be analyzed [89]. In case of vasa previa, the waveforms obtained with the Doppler will show fetal blood flow [89, 99]. As the vessel could also be a loop of the umbilical cord close to the cervix, this has to be distinguished from membranous vasa previa [89, 99].

MRI

Although MRI does offer proper evaluation of the placenta in relation to the cervix, transvaginal ultrasound is in general sufficient for diagnosis.

Umbilical Cord

Umbilical Cord Development and Sonography

The rudimentary umbilical cord develops between the 4th and 8th week of gestation. Tissue from the body stalk (containing two umbilical arteries, one vein, and the allantois), the omphalomesenteric duct, and the umbilical coelom is enveloped by the expanding amnion. The umbilical arteries arise originally from the primitive dorsal aorta. By the end of the 5th week of gestation, blood flow is established (due to cardiac contractions). After birth, the patent internal, intra-abdominal, bodily part of the umbilical arteries becomes the internal iliac and superior vesical arteries. The distal parts collapse due to loss of function and become the medial umbilical ligaments. Originally two veins develop but the right vein obliterates around 6th week of gestation and regresses, the left one persisting [26, 118]. The umbilical cord can be seen on ultrasound from 42 days of gestation as the connection between the trophoblast mass and fetus as a ropelike echogenic structure [36]. Pulsations can be visualized on ultrasound from the moment the fetal heart starts contracting. The umbilical vessels are surrounded by Wharton jelly, this jelly consists of connective tissue with a generous amount of extracellular matrix, mainly consisting of hydrophilic proteoglycans and hyalurac acid. The umbilical vessels are protected by the Wharton jelly from tearing and compression due to the achieved elasticity and strength [38]. The umbilical vessels have a tortuous course. In advanced gestation it can be difficult to assess the complete umbilical cord due to its mobility, the size and position of the fetus and placenta, and amniotic fluid volume which forms the contrast for the intrauterine contents [72]. Modern ultrasound facilitates assessment of the umbilical artery: color Doppler can visualize vascular alterations and 3D HD Doppler flow provides further information including the direction of the flow, which results in a more sensitive technique for lesions such as umbilical knots [107].

Pathology of the Umbilical Cord (Chap. 27)

During pregnancy the fetus is fully dependent on umbilical cord for oxygen- and nutrient-rich blood supply. Any abnormalities in the umbilical cord are associated with either abnormalities in fetal development, or in complicated delivery outcomes [50]. With improved ultrasound techniques and more attention to the placenta and umbilical cord many of these abnormalities can be diagnosed prenatally.

Abnormality in Number of Vessels

When an umbilical artery undergoes atresia, aplasia, or agenesis, this results in a single umbilical artery (SUA), and the left artery is most often affected and absent [101]. SUA is more often seen in association with a range of congenital malformations, fetal growth restriction, and aneuploidy. Isolated SUA generally has a good prognosis.

It is estimated that single umbilical artery (SUA) affects up to 0.5–1% of pregnancies [91]. The majority of SUAs are isolated, and only a minority of fetuses has additional ultrasound findings of congenital anomalies [127, 128]. Using ultrasound, SUA can be reliably detected from around 13 weeks of gestation [42], although most cases of SUA will be discovered during routine anomaly scans at 20 weeks.

Persistent Right Umbilical Vein

Persistence of the right umbilical vein in the fetus is rare and associated with congenital malformations, mainly cardiac. The left umbilical vein then occludes and no abnormalities can be visualized in the umbilical cord. The persistent vessel is part of the usual fetal intra-abdominal umbilical venous connection that usually regresses. The persistent right umbilical vein can be seen on routine ultrasound in the transverse section of the fetal abdomen. The umbilical vein runs laterally, to the right of the gallbladder. When the persistent vein concerns the intrahepatic version, it connects to the right portal vein that runs toward the stomach. When it concerns the extra hepatic version the right umbilical vein may drain into the right atrium, in the inferior vena cava (infra-cardiac) or iliac veins [76].

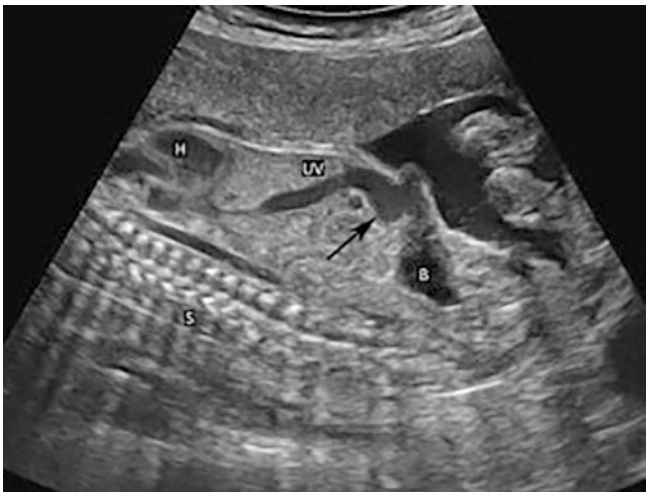

Fig. 32.12 Ultrasound image of umbilical vein varix. Showing the longitudinal course of the umbilical vein. UV umbilical vein, B bladder, H heart, S spine, arrow: umbilical vein varix [2]

Umbilical Vein Varix

Umbilical vein varices are rare (Fig. 32.12); these vein varices are mostly found intra-abdominally, although some cases of extra-abdominal varices have been described [16, 22, 33]. On ultrasound examination, an intra-abdominal vein varix mostly appears as a cystic mass [33]. To exclude other causes of possible intra-abdominal cysts Doppler ultrasound shows a venous type flow in the cyst [2]. Several definitions have been used including a diameter exceeding 9 mm and/or a diameter of the sub-hepatic segment of the upper umbilical vein exceeding 50% of the diameter of the intra-hepatic segment [2]. Using ultrasound, it is advised to differentiate a specific form of the intra-abdominal umbilical vein varix, the umbilical vein that ends in the extra-hepatic portal system. This form of umbilical vein varix is often characterized by a large diameter, twice as wide in combination with turbulence [2].

Cord Insertion Abnormalities

Umbilical cord insertion is optimally located at the center of the placenta, and insertion site can best be visualized using color Doppler [34]. A marginal insertion is seen when the insertion is located at a distance of less than 2 cm from the edge, with all subsequent branching vessels in the placenta. A velamentous insertion can be visualized by color Doppler when the cord appears to directly insert on the uterine wall beyond the placental disc and branching vessels are submembranous [130]. A marginal insertion may develop to a velamentous insertion with advancing pregnancy [102]. Ultrasonography is very specific (100%) but only moderately sensitive for determination of abnormal placental cord insertion site [34].

Cord Coiling Abnormalities (Both Hyper- and Hypo-Coiling)

The vessels in the umbilical cord have a tortuous course; the arteries entangle the vein, usually resulting in a left sided twist/coil. Normal coiling indexes are described to be between 0.19 and 0.44 coils per centimeter. Interestingly the antenatal coiling index does not correspond well with the postnatal coiling index, presumably because postnatally there is no blood flow but also due to the variability of coiling throughout the length of the cord [30]. The fetal blood flow distends the cord resulting in a tighter apparent coiling of the vascular helix. Despite the slight antenatal–postnatal difference the association with adverse outcomes is reported for both hypo- and hyper-coiling in both antenatal and postnatal measured indexes [111]. A term cord is around 17-mm thick and a cord with a diameter less than 10 mm at term is considered thin and is associated with small for gestational age and postdates [72].

Cord Tumors

Cord tumors can be well assessed by ultrasound at all stages of pregnancy. Most often cysts are observed. Depending on the contents of the cysts, usually fluids, they are more echo lucent than their surroundings. Cysts are usually a result of embryonic remnants and are located proximal to the fetus. They usually resolve spontaneously but can be associated with adverse effects specifically when located close to the fetus (usually allantoic cysts) or the placenta [43, 108]. Pseudocysts can be visualized at any location along the umbilical cord and are caused by degeneration or edema of Whartons jelly and not covered by epithelium [72].

Early in pregnancy a physiologic umbilical hernia may exist that resolves before the 12th week of gestation due to intestinal rotation. Herniation of abdominal organs after 12 weeks is abnormal and represents omphalocele, covered by umbilical epithelium and appearing as an echo dense protuberance into the umbilical cord. Gastroschisis may appear somewhat similar sonographically but represents herniation of the abdominal organs, commonly the intestines, into the amniotic cavity through a Para umbilical defect, usually located right from the umbilical cord; gastroschisis contents are not covered by umbilical cord.

Novel and Potential Future Placental Imaging Modalities

MicroCT

Micro computed CT is a technique which allows extremely high-resolution X-ray-based imaging of ex vivo tissues. With

the use of vascular contrast and micro CT investigation of the placenta has been described, providing extremely high-resolution three-dimensional imaging. Due to the limitations of the technique itself and the need for X-rays, this is unlikely to represent an image modality that could be used antenatally but due to the high resolution could provide novel insights into underlying consent or pathological mechanisms following postdelivery imaging.

Photoacoustic Imaging

Similarly, using novel types of high-frequency probes in an ex vivo setting, photoacoustic imaging can provide novel anatomical visualization of the placental vasculature. At present this approach has only been demonstrated in principle but has the potential to be developed for use prior to delivery in selecting cases in the future.

References

1. Alanjari A, Wright E, Keating S, Ryan G, Kingdom J. Prenatal diagnosis, clinical outcomes, and associated pathology in pregnancies complicated by massive subchorionic thrombohematoma (Breus' mole). Prenat Diagn. 2013;33(10):973–8.
2. Beraud E, Rozel C, Milon J, Darnault P. Umbilical vein varix: importance of ante- and post-natal monitoring by ultrasound. Diagn Interv Imaging. 2015;96(1):21–6.
3. Bhide A, Acharya G, Bilardo CM, Brezinka C, Cafici D, Hernandez-Andrade E, Kalache K, Kingdom J, Kiserud T, Lee W, Lees C, Leung KY, Malinger G, Mari G, Prefumo F, Sepulveda W, Trudinger B. ISUOG practice guidelines: use of Doppler ultrasonography in obstetrics. Ultrasound Obstet Gynecol. 2013;41(2):233–9.
4. Gratacos E, Lewi L, Munoz B, Acosta-Rojas R, Hernandez-Andrade E, Martinez JM, Carreras E, Deprest J. A classification system for selective intrauterine growth restriction in monochorionic pregnancies according to umbilical artery Doppler flow in the smaller twin. Ultrasound Obstet Gynecol. 2007;30(1):28–34.
5. Hata T, Tanaka H, Noguchi J, Hata K. Three-dimensional ultrasound evaluation of the placenta. Placenta. 2011;32(2):105–15.
6. Ishibashi H, Miyamoto M, Shinmoto H, Soga S, Matsuura H, Kakimoto S, Iwahashi H, Sakamoto T, Hada T, Suzuki R, Takano M. The use of magnetic resonance imaging to predict placenta previa with placenta accreta spectrum. Acta Obstet Gynecol Scand. 2020;99:1657–65.
7. Linduska N, Messerschmidt A, Dekan S, Brugger PC, Weber M, Pollak A, Prayer D. Placental magnetic resonance imaging in monochorionic twin pregnancies. J Matern Fetal Neonatal Med. 2012;25(8):1419–22.
8. Abaci Turk E, Stout JN, Ha C, Luo J, Gagoski B, Yetisir F, Golland P, Wald LL, Adalsteinsson E, Robinson JN, Roberts DJ, Barth WH Jr, Grant PE. Placental MRI: developing accurate quantitative measures of oxygenation. Top Magn Reson Imaging. 2019;28(5):285–97.
9. Abramowicz JS, Barnett SB, Duck FA, Edmonds PD, Hynynen KH, Ziskin MC. Fetal thermal effects of diagnostic ultrasound. J Ultrasound Med. 2008;27(4):541–59; quiz 560-543.
10. Abramowicz JS, Sheiner E. Ultrasound of the placenta: a systematic approach. Part I: imaging. Placenta. 2008;29(3):225–40.
11. Adams HP, Malloy J. Cystic placentomegaly on a second-trimester ultrasound. JAAPA. 2018;31(1):36–40.
12. Bajaj SK, Misra R, Gupta R, Nisha B, Thukral BB. Complete hydatidiform mole with coexisting twin fetus: usefulness of MRI in management planning. J Obstet Gynaecol India. 2014;64(Suppl 1):9–13.
13. Baschat AA. Fetal growth restriction - from observation to intervention. J Perinat Med. 2010;38(3):239–46.
14. Benson CB, Genest DR, Bernstein MR, Soto-Wright V, Goldstein DP, Berkowitz RS. Sonographic appearance of first trimester complete hydatidiform moles. Ultrasound Obstet Gynecol. 2000;16(2):188–91.
15. Blaicher W, Brugger PC, Mittermayer C, Schwindt J, Deutinger J, Bernaschek G, Prayer D. Magnetic resonance imaging of the normal placenta. Eur J Radiol. 2006;57(2):256–60.
16. Bouzid A, Karmous N, Trabelsi H, Mkaouar L, Mourali M. Fetal intra-abdominal umbilical vein varix: a case report and literature review. Gynecol Obstet. 2016;6(5):420–2.
17. Brown BP, Meyers ML. Placental magnetic resonance imaging part II: placenta accreta spectrum. Pediatr Radiol. 2020;50(2):275–84.
18. Brown RE. Ultrasonic localization of the placenta. Radiology. 1967;89(5):828–33.
19. Bulas D, Egloff A. Benefits and risks of MRI in pregnancy. Semin Perinatol. 2013;37(5):301–4.
20. Burton GJ, Woods AW, Jauniaux E, Kingdom JC. Rheological and physiological consequences of conversion of the maternal spiral arteries for uteroplacental blood flow during human pregnancy. Placenta. 2009;30(6):473–82.
21. Campbell S. A short history of sonography in obstetrics and gynaecology. Facts Views Vis Obgyn. 2013;5(3):213–29.
22. Cassidy-Vu L, Clark S, Cuka N. Extra-abdominal umbilical vein varix in a newborn. BMJ Case Rep. 2019;12(5):e227424.
23. Cavoretto P, Cioffi R, Mangili G, Petrone M, Bergamini A, Rabaiotti E, Valsecchi L, Candiani M, Seckl MJ. A pictorial ultrasound essay of gestational trophoblastic disease. J Ultrasound Med. 2020;39(3):597–613.
24. Chaoui R, Jeanty P, Paladini D. Ultrasound in obstetrics and gynecology: a practical approach.
25. Chartier AL, Bouvier MJ, McPherson DR, Stepenosky JE, Taysom DA, Marks RM. The safety of maternal and fetal MRI at 3 T. AJR Am J Roentgenol. 2019;213(5):1170–3.
26. Cochard LR. Netter's atlas of human embryology. Philadelphia, Saunders; 2002.
27. Cooley SM, Donnelly JC, Walsh T, McMahon C, Gillan J, Geary MP. The correlation of ultrasonographic placental architecture with placental histology in the low-risk primigravid population. J Perinat Med. 2013;41(5):505–9.
28. D'Antonio F, Bhide A. Early pregnancy assessment in multiple pregnancies. Best Pract Res Clin Obstet Gynaecol. 2014;28(2):201–14.
29. Damadian R. Tumor detection by nuclear magnetic resonance. Science. 1971;171(3976):1151–3.
30. De Laat MW, Franx A, Nikkels PG, Visser GH. Prenatal ultrasonographic prediction of the umbilical coiling index at birth and adverse pregnancy outcome. Ultrasound Obstet Gynecol. 2006;28(5):704–9.
31. De Paepe ME, Shapiro S, Greco D, Luks VL, Abellar RG, Luks CH, Luks FI. Placental markers of twin-to-twin transfusion syndrome in diamniotic-monochorionic twins: a morphometric analysis of deep artery-to-vein anastomoses. Placenta. 2010;31(4):269–76.
32. Denbow ML, Cox P, Taylor M, Hammal DM, Fisk NM. Placental angioarchitecture in monochorionic twin pregnancies: relationship to fetal growth, fetofetal transfusion syndrome, and pregnancy outcome. Am J Obstet Gynecol. 2000;182(2):417–26.
33. di Pasquo E, Kuleva M, O'Gorman N, Ville Y, Salomon LJ. Fetal intra-abdominal umbilical vein varix: retrospective cohort study

and systematic review and meta-analysis. Ultrasound Obstet Gynecol. 2018;51(5):580–5.
34. Di Salvo DN, Benson CB, Laing FC, Brown DL, Frates MC, Doubilet PM. Sonographic evaluation of the placental cord insertion site. AJR Am J Roentgenol. 1998;170(5):1295–8.
35. Donald I, Macvicar J, Brown TG. Investigation of abdominal masses by pulsed ultrasound. Lancet. 1958;1(7032):1188–95.
36. Dudiak CM, Salomon CG, Posniak HV, Olson MC, Flisak ME. Sonography of the umbilical cord. Radiographics. 1995;15(5):1035–50.
37. El-Agwany AS. Large subchorionic hematoma: Breus' mole. J Med Ultrasound. 2017;25(4):248–50.
38. Ferguson VL, Dodson RB. Bioengineering aspects of the umbilical cord. Eur J Obstet Gynecol Reprod Biol. 2009;144(Suppl 1):S108–13.
39. Fick AL, Feldstein VA, Norton ME, Wassel Fyr C, Caughey AB, Machin GA. Unequal placental sharing and birth weight discordance in monochorionic diamniotic twins. Am J Obstet Gynecol. 2006;195(1):178–83.
40. Frias AE. Placenta imaging project (PIP); 2016.
41. Fung TY, To KF, Sahota DS, Chan LW, Leung TY, Lau TK. Massive subchorionic thrombohematoma: a series of 10 cases. Acta Obstet Gynecol Scand. 2010;89(10):1357–61.
42. Geipel A, Germer U, Welp T, Schwinger E, Gembruch U. Prenatal diagnosis of single umbilical artery: determination of the absent side, associated anomalies, Doppler findings and perinatal outcome. Ultrasound Obstet Gynecol. 2000;15(2):114–7.
43. Ghezzi F, Raio L, Di Naro E, Franchi M, Cromi A, Durig P. Single and multiple umbilical cord cysts in early gestation: two different entities. Ultrasound Obstet Gynecol. 2003;21(3):215–9.
44. Gill RW, Trudinger BJ, Garrett WJ, Kossoff G, Warren PS. Fetal umbilical venous flow measured in utero by pulsed Doppler and B-mode ultrasound. I. Normal pregnancies. Am J Obstet Gynecol. 1981;139(6):720–5.
45. Glantz C, Purnell L. Clinical utility of sonography in the diagnosis and treatment of placental abruption. J Ultrasound Med. 2002;21(8):837–40.
46. Gordijn SJ, Beune IM, Thilaganathan B, Papageorghiou A, Baschat AA, Baker PN, Silver RM, Wynia K, Ganzevoort W. Consensus definition of fetal growth restriction: a Delphi procedure. Ultrasound Obstet Gynecol. 2016;48(3):333–9.
47. Groene SG, Tollenaar LSA, Slaghekke F, Middeldorp JM, Haak M, Oepkes D, Lopriore E. Placental characteristics in monochorionic twins with selective intrauterine growth restriction in relation to the umbilical artery Doppler classification. Placenta. 2018;71:1–5.
48. Harris RD, Cho C, Wells WA. Sonography of the placenta with emphasis on pathological correlation. Semin Ultrasound CT MR. 1996;17(1):66–89.
49. Harris RD, Simpson WA, Pet LR, Marin-Padilla M, Crow HC. Placental hypoechoic-anechoic areas and infarction: sonographic-pathologic correlation. Radiology. 1990;176(1):75–80.
50. Hasegawa J. Ultrasound screening of umbilical cord abnormalities and delivery management. Placenta. 2018;62:66–78.
51. Heinrichs WL, Fong P, Flannery M, Heinrichs SC, Crooks LE, Spindle A, Pedersen RA. Midgestational exposure of pregnant BALB/c mice to magnetic resonance imaging conditions. Magn Reson Imaging. 1988;6(3):305–13.
52. Hoskins P, Martin K, Thrush A. Diagnostic ultrasound: physics and equipment. Cambridge: Cambridge University Press; 2010.
53. Houston LE, Odibo AO, Macones GA. The safety of obstetrical ultrasound: a review. Prenat Diagn. 2009;29(13):1204–12.
54. Imafuku H, Miyahara Y, Ebina Y, Yamada H. Ultrasound and MRI findings of twin pregnancies with complete hydatidiform mole and coexisting normal fetus: two case reports. Kobe J Med Sci. 2018;64(1):E1–5.
55. Inubashiri E, Deguchi K, Abe K, Saitou A, Watanabe Y, Akutagawa N, Kuroki K, Sugawara M, Maeda N. Three-dimensional high-definition flow in the diagnosis of placental lakes. J Med Ultrason (2001). 2014;41(4):491–4.
56. Jaimes C, Delgado J, Cunnane MB, Hedrick HL, Adzick NS, Gee MS, Victoria T. Does 3-T fetal MRI induce adverse acoustic effects in the neonate? A preliminary study comparing postnatal auditory test performance of fetuses scanned at 1.5 and 3 T. Pediatr Radiol. 2019;49(1):37–45.
57. Jauniaux E, Avni FE, Elkhazen N, Wilkin P, Hustin J. Morphologic study of ultrasonic placental anomalies in the second half of pregnancy. J Gynecol Obstet Biol Reprod (Paris). 1989;18(5):601–13.
58. Jauniaux E, Ayres-de-Campos D, Diagnosis FPA, P. Management Expert Consensus. FIGO consensus guidelines on placenta accreta spectrum disorders: introduction. Int J Gynaecol Obstet. 2018;140(3):261–4.
59. Jauniaux E, Campbell S. Antenatal diagnosis of placental infarcts by ultrasonography. J Clin Ultrasound. 1991;19(1):58–61.
60. Jauniaux E, Memtsa M, Johns J, Ross JA, Jurkovic D. New insights in the pathophysiology of complete hydatidiform mole. Placenta. 2018;62:28–33.
61. Jauniaux E, Moffett A, Burton GJ. Placental implantation disorders. Obstet Gynecol Clin North Am. 2020;47(1):117–32.
62. Jha P, Masselli G, Ohliger MA, Poder L. Nonfetal imaging during pregnancy: placental disease. Radiol Clin North Am. 2020;58(2):381–99.
63. Jha P, Poder L, Bourgioti C, Bharwani N, Lewis S, Kamath A, Nougaret S, Soyer P, Weston M, Castillo RP, Kido A, Forstner R, Masselli G. Society of Abdominal Radiology (SAR) and European Society of Urogenital Radiology (ESUR) joint consensus statement for MR imaging of placenta accreta spectrum disorders. Eur Radiol. 2020;30(5):2604–15.
64. Jiao L, Ghorani E, Sebire NJ, Seckl MJ. Intraplacental choriocarcinoma: systematic review and management guidance. Gynecol Oncol. 2016;141(3):624–31.
65. Kellow ZS, Feldstein VA. Ultrasound of the placenta and umbilical cord: a review. Ultrasound Q. 2011;27(3):187–97.
66. Khalil A. Modified diagnostic criteria for twin-to-twin transfusion syndrome prior to 18 weeks' gestation: time to change? Ultrasound Obstet Gynecol. 2017;49(6):804–5.
67. Khalil A, Rodgers M, Baschat A, Bhide A, Gratacos E, Hecher K, Kilby MD, Lewi L, Nicolaides KH, Oepkes D, Raine-Fenning N, Reed K, Salomon LJ, Sotiriadis A, Thilaganathan B, Ville Y. ISUOG practice guidelines: role of ultrasound in twin pregnancy. Ultrasound Obstet Gynecol. 2016;47(2):247–63.
68. Khong TY, Mooney EE, Ariel I, Balmus NC, Boyd TK, Brundler MA, Derricott H, Evans MJ, Faye-Petersen OM, Gillan JE, Heazell AE, Heller DS, Jacques SM, Keating S, Kelehan P, Maes A, McKay EM, Morgan TK, Nikkels PG, Parks WT, Redline RW, Scheimberg I, Schoots MH, Sebire NJ, Timmer A, Turowski G, van der Voorn JP, van Lijnschoten I, Gordijn SJ. Sampling and definitions of placental lesions: Amsterdam placental workshop group consensus statement. Arch Pathol Lab Med. 2016;140(7):698–713.
69. Kibel M, Kahn M, Sherman C, Kingdom J, Zaltz A, Barrett J, Melamed N. Placental abnormalities differ between small for gestational age fetuses in dichorionic twin and singleton pregnancies. Placenta. 2017;60:28–35.
70. Kilcoyne A, Shenoy-Bhangle AS, Roberts DJ, Sisodia RC, Gervais DA, Lee SI. MRI of placenta accreta, placenta increta, and placenta percreta: pearls and pitfalls. AJR Am J Roentgenol. 2017;208(1):214–21.
71. Kingdom J, Huppertz B, Seaward G, Kaufmann P. Development of the placental villous tree and its consequences for fetal growth. Eur J Obstet Gynecol Reprod Biol. 2000;92(1):35–43.
72. Krzyzanowski A, Kwiatek M, Geca T, Stupak A, Kwasniewska A. Modern ultrasonography of the umbilical cord: prenatal diag-

nosis of umbilical cord abnormalities and assessement of fetal wellbeing. Med Sci Monit. 2019;25:3170–80.
73. Lax A, Prince MR, Mennitt KW, Schwebach JR, Budorick NE. The value of specific MRI features in the evaluation of suspected placental invasion. Magn Reson Imaging. 2007;25(1):87–93.
74. Lewi L, Gucciardo L, Huber A, Jani J, Van Mieghem T, Done E, Cannie M, Gratacos E, Diemert A, Hecher K, Lewi P, Deprest J. Clinical outcome and placental characteristics of monochorionic diamniotic twin pairs with early- and late-onset discordant growth. Am J Obstet Gynecol. 2008;199(5):511 e511–7.
75. Leyendecker JR, DuBose M, Hosseinzadeh K, Stone R, Gianini J, Childs DD, Snow AN, Mertz H. MRI of pregnancy-related issues: abnormal placentation. AJR Am J Roentgenol. 2012;198(2):311–20.
76. Lide B, Lindsley W, Foster MJ, Hale R, Haeri S. Intrahepatic persistent right umbilical vein and associated outcomes: a systematic review of the literature. J Ultrasound Med. 2016;35(1):1–5.
77. Lin LH, Polizio R, Fushida K, Francisco RPV. Imaging in gestational trophoblastic disease. Semin Ultrasound CT MR. 2019;40(4):332–49.
78. Linduska N, Dekan S, Messerschmidt A, Kasprian G, Brugger PC, Chalubinski K, Weber M, Prayer D. Placental pathologies in fetal MRI with pathohistological correlation. Placenta. 2009;30(6):555–9.
79. Lopriore E, Pasman SA, Klumper FJ, Middeldorp JM, Walther FJ, Oepkes D. Placental characteristics in growth-discordant monochorionic twins: a matched case-control study. Placenta. 2012;33(3):171–4.
80. Lopriore E, Slaghekke F, Oepkes D, Middeldorp JM, Vandenbussche FP, Walther FJ. Hematological characteristics in neonates with twin anemia-polycythemia sequence (TAPS). Prenat Diagn. 2010;30(3):251–5.
81. Lum M, Tsiouris AJ. MRI safety considerations during pregnancy. Clin Imaging. 2020;62:69–75.
82. Magin RL, Lee JK, Klintsova A, Carnes KI, Dunn F. Biological effects of long-duration, high-field (4 T) MRI on growth and development in the mouse. J Magn Reson Imaging. 2000;12(1):140–9.
83. Marycz K, Kornicka K, Rocken M. Static magnetic field (SMF) as a regulator of stem cell fate - new perspectives in regenerative medicine arising from an underestimated tool. Stem Cell Rev Rep. 2018;14(6):785–92.
84. Messerschmidt A, Baschat A, Linduska N, Kasprian G, Brugger PC, Bauer A, Weber M, Prayer D. Magnetic resonance imaging of the placenta identifies placental vascular abnormalities independently of Doppler ultrasound. Ultrasound Obstet Gynecol. 2011;37(6):717–22.
85. Mevissen M, Buntenkotter S, Loscher W. Effects of static and time-varying (50-Hz) magnetic fields on reproduction and fetal development in rats. Teratology. 1994;50(3):229–37.
86. Mifsud W, Sebire NJ. Placental pathology in early-onset and late-onset fetal growth restriction. Fetal Diagn Ther. 2014;36(2):117–28.
87. Miyagi M, Kinjo T, Mekaru K, Nitta H, Masamoto H, Aoki Y. Massive subchorionic thrombohematoma (Breus' mole) associated with fetal growth restriction, oligohydramnios, and intrauterine fetal death. Case Rep Obstet Gynecol. 2019;2019:9510936.
88. Moore RJ, Strachan BK, Tyler DJ, Duncan KR, Baker PN, Worthington BS, Johnson IR, Gowland PA. In utero perfusing fraction maps in normal and growth restricted pregnancy measured using IVIM echo-planar MRI. Placenta. 2000;21(7):726–32.
89. Moshiri M, Zaidi SF, Robinson TJ, Bhargava P, Siebert JR, Dubinsky TJ, Katz DS. Comprehensive imaging review of abnormalities of the umbilical cord. Radiographics. 2014;34(1):179–96.
90. Muhler MR, Clement O, Salomon LJ, Balvay D, Autret G, Vayssettes C, Cuenod CA, Siauve N. Maternofetal pharmacokinetics of a gadolinium chelate contrast agent in mice. Radiology. 2011;258(2):455–60.
91. Murphy-Kaulbeck L, Dodds L, Joseph KS, Van den Hof M. Single umbilical artery risk factors and pregnancy outcomes. Obstet Gynecol. 2010;116(4):843–50.
92. Nayeri UA, West AB, Grossetta Nardini HK, Copel JA, Sfakianaki AK. Systematic review of sonographic findings of placental mesenchymal dysplasia and subsequent pregnancy outcome. Ultrasound Obstet Gynecol. 2013;41(4):366–74.
93. Nicolaides KH, Rizzo G, Hecher K. Doppler in obstetrics; 2002.
94. Nikkels PG, Hack KE, van Gemert MJ. Pathology of twin placentas with special attention to monochorionic twin placentas. J Clin Pathol. 2008;61(12):1247–53.
95. Novak Z, Thurmond AS, Ross PL, Jones MK, Thornburg KL, Katzberg RW. Gadolinium-DTPA transplacental transfer and distribution in fetal tissue in rabbits. Invest Radiol. 1993;28(9):828–30.
96. Nowak PM, Nardozza LM, Araujo Junior E, Rolo LC, Moron AF. Comparison of placental volume in early pregnancy using multiplanar and VOCAL methods. Placenta. 2008;29(3):241–5.
97. Nyberg DA, Cyr DR, Mack LA, Wilson DA, Shuman WP. Sonographic spectrum of placental abruption. AJR Am J Roentgenol. 1987;148(1):161–4.
98. Oh KY, Roberts VH, Schabel MC, Grove KL, Woods M, Frias AE. Gadolinium chelate contrast material in pregnancy: fetal biodistribution in the nonhuman primate. Radiology. 2015;276(1):110–8.
99. Oyelese Y. Placenta, umbilical cord and amniotic fluid: the not-less-important accessories. Clin Obstet Gynecol. 2012;55(1):307–23.
100. Oyelese Y, Ananth CV. Placental abruption. Obstet Gynecol. 2006;108(4):1005–16.
101. Predanic M. Sonographic assessment of the umbilical cord. Ultrasound Rev Obstet Gynecol. 2005;5(2):105–10.
102. Pretorius DH, Chau C, Poeltler DM, Mendoza A, Catanzarite VA, Hollenbach KA. Placental cord insertion visualization with prenatal ultrasonography. J Ultrasound Med. 1996;15(8):585–93.
103. Ray JG, Vermeulen MJ, Bharatha A, Montanera WJ, Park AL. Association between MRI exposure during pregnancy and fetal and childhood outcomes. JAMA. 2016;316(9):952–61.
104. Reis NS, Brizot ML, Schultz R, Nomura RM, Zugaib M. Placental lakes on sonographic examination: correlation with obstetric outcome and pathologic findings. J Clin Ultrasound. 2005;33(2):67–71.
105. Roberts D, Gates S, Kilby M, Neilson JP. Interventions for twin-twin transfusion syndrome: a Cochrane review. Ultrasound Obstet Gynecol. 2008;31(6):701–11.
106. Roberts D, Neilson JP, Kilby MD, Gates S. Interventions for the treatment of twin-twin transfusion syndrome. Cochrane Database Syst Rev. 2014;(1):CD002073.
107. Rodriguez N, Angarita AM, Casasbuenas A, Sarmiento A. Three-dimensional high-definition flow imaging in prenatal diagnosis of a true umbilical cord knot. Ultrasound Obstet Gynecol. 2012;39(2):245–6.
108. Ross JA, Jurkovic D, Zosmer N, Jauniaux E, Hacket E, Nicolaides KH. Umbilical cord cysts in early pregnancy. Obstet Gynecol. 1997;89(3):442–5.
109. Salomon LJ, Bernard JP, Millischer AE, Sonigo P, Brunelle F, Boddaert N, Ville Y. MRI and ultrasound fusion imaging for prenatal diagnosis. Am J Obstet Gynecol. 2013;209(2):148 e141–9.
110. Scherjon SA, Smolders-DeHaas H, Kok JH, Zondervan HA. The "brain-sparing" effect: antenatal cerebral Doppler findings in relation to neurologic outcome in very preterm infants. Am J Obstet Gynecol. 1993;169(1):169–75.
111. Sebire NJ, Sepulveda W. Correlation of placental pathology with prenatal ultrasound findings. J Clin Pathol. 2008;61(12):1276–84.

112. Seckl MJ, Sebire NJ, Berkowitz RS. Gestational trophoblastic disease. Lancet. 2010;376(9742):717–29.
113. Shaaban AM, Rezvani M, Haroun RR, Kennedy AM, Elsayes KM, Olpin JD, Salama ME, Foster BR, Menias CO. Gestational trophoblastic disease: clinical and imaging features. Radiographics. 2017;37(2):681–700.
114. Siauve N, Chalouhi GE, Deloison B, Alison M, Clement O, Ville Y, Salomon LJ. Functional imaging of the human placenta with magnetic resonance. Am J Obstet Gynecol. 2015;213(4 Suppl):S103–14.
115. Sirotkina M, Douroudis K, Westgren M, Papadogiannakis N. Association of chorangiomas to hypoxia-related placental changes in singleton and multiple pregnancy placentas. Placenta. 2016;39:154–9.
116. Slaghekke F, Kist WJ, Oepkes D, Pasman SA, Middeldorp JM, Klumper FJ, Walther FJ, Vandenbussche FP, Lopriore E. Twin anemia-polycythemia sequence: diagnostic criteria, classification, perinatal management and outcome. Fetal Diagn Ther. 2010;27(4):181–90.
117. Smith FW, Adam AH, Phillips WD. NMR imaging in pregnancy. Lancet. 1983;1(8314–5):61–2.
118. Spurway J, Logan P, Pak S. The development, structure and blood flow within the umbilical cord with particular reference to the venous system. Australas J Ultrasound Med. 2012;15(3):97–102.
119. Stevenson GN, Noble JA, Welsh AW, Impey L, Collins SL. Automated visualization and quantification of spiral artery blood flow entering the first-trimester placenta, using 3-D power Doppler ultrasound. Ultrasound Med Biol. 2018;44(3):522–31.
120. Strizek B, Jani JC, Mucyo E, De Keyzer F, Pauwels I, Ziane S, Mansbach AL, Deltenre P, Cos T, Cannie MM. Safety of MR imaging at 1.5 T in fetuses: a retrospective case-control study of birth weights and the effects of acoustic noise. Radiology. 2015;275(2):530–7.
121. Suzuki S. Clinical significance of pregnancies with circumvallate placenta. J Obstet Gynaecol Res. 2008;34(1):51–4.
122. Taniguchi H, Aoki S, Sakamaki K, Kurasawa K, Okuda M, Takahashi T, Hirahara F. Circumvallate placenta: associated clinical manifestations and complications-a retrospective study. Obstet Gynecol Int. 2014;2014:986230.
123. Tollenaar LS, Zhao DP, Middeldorp JM, Slaghekke F, Oepkes D, Lopriore E. Color difference in placentas with twin anemia-polycythemia sequence: an additional diagnostic criterion? Fetal Diagn Ther. 2016;40(2):123–7.
124. Tollenaar LSA, Zhao DP, Middeldorp JM, Oepkes D, Slaghekke F, Lopriore E. Can color difference on the maternal side of the placenta distinguish between acute peripartum twin-twin transfusion syndrome and twin anemia-polycythemia sequence? Placenta. 2017;57:189–93.
125. Ulker V, Aslan H, Gedikbasi A, Yararbas K, Yildirim G, Yavuz E. Placental mesenchymal dysplasia: a rare clinicopathologic entity confused with molar pregnancy. J Obstet Gynaecol. 2013;33(3):246–9.
126. Weiss G, Sundl M, Glasner A, Huppertz B, Moser G. The trophoblast plug during early pregnancy: a deeper insight. Histochem Cell Biol. 2016;146(6):749–56.
127. Wiegand S, McKenna DS, Croom C, Ventolini G, Sonek JD, Neiger R. Serial sonographic growth assessment in pregnancies complicated by an isolated single umbilical artery. Am J Perinatol. 2008;25(3):149–52.
128. Willner NT, Wainstock T, Walfisch A, Sheiner E, Landau D, Beharier O. Isolated single umbilical artery as a risk factor for urinary tract infections in childhood. Am J Perinatol. 2021;38:597–601.
129. Wolf H, Oosting H, Treffers PE. Second-trimester placental volume measurement by ultrasound: prediction of fetal outcome. Am J Obstet Gynecol. 1989;160(1):121–6.
130. Woodward PJ, Kennedy A, Sohaey R. Diagnostic imaging: obstetrics. Philadelphia, Elsevier; 2016.
131. Zalud I, Shaha S. Evaluation of the utero-placental circulation by three-dimensional Doppler ultrasound in the second trimester of normal pregnancy. J Matern Fetal Neonatal Med. 2007;20(4):299–305.